



Research Article

Enhanced precipitation has driven the evolution of subtropical evergreen broad-leaved forests in eastern China since the early Miocene: Evidence from ring-cupped oaks

Dong-Mei Jin^{1†*} , Quan Yuan^{1,2†}, Xi-Ling Dai², Gregor Kozłowski^{1,3,4}, and Yi-Gang Song^{1*} ¹Eastern China Conservation Centre for Wild Endangered Plant Resources, Shanghai Chenshan Botanical Garden, Shanghai 201602, China²College of Life Sciences, Shanghai Normal University, Shanghai 200234, China³Department of Biology and Botanic Garden, University of Fribourg, Fribourg 1700, Switzerland⁴Natural History Museum Fribourg, Fribourg 1700, Switzerland

†These authors contributed equally to this study.

*Authors for correspondence. Dong-Mei Jin. E-mail: jindongmei@csnbgsh.cn; Yi-Gang Song. E-mail: ygsong@cemps.ac.cn

Received 2 February 2023; Revised 3 August 2023; Accepted 16 August 2023

Abstract Subtropical evergreen broad-leaved forest (EBLF) is the predominant vegetation type in eastern China. However, the majority of the region it covers in eastern China was an arid area during the Paleogene. The temporal history and essential factors involved in the evolution of subtropical EBLFs in eastern China remain enigmatic. Here we report on the niche evolution of *Quercus* section *Cyclobalanopsis*, which appeared in south China and Japan during the Eocene and became a dominant component of subtropical EBLFs since the Miocene in eastern Asia, using integrative analysis of occurrences, climate data and a dated phylogeny of 35 species in *Cyclobalanopsis*. Species within clades *Cyclobalanoides*, *Lamellosa*, and *Helferiana* mainly inhabit in the Himalaya–Hengduan region, adapting to a plateau climate, while species within the other clades mainly live in eastern China under the control of the East Asian monsoon. Reconstructed history showed that significant divergence of climatic tolerance in *Cyclobalanopsis* began around 19 million years ago (Ma) in the early Miocene. Simultaneously, the disparity in precipitation of wettest/warmest quarter and annual precipitation was markedly enhanced in *Cyclobalanopsis*, especially in the recent eastern clades. During the Miocene, the marked radiation of *Cyclobalanopsis* and many other dominant taxa of subtropical EBLFs strongly suggest the rapid formation and expansion of subtropical EBLFs in eastern China. Our research highlights that the intensification of the East Asian monsoon and subsequent occupation of new niches by the ancient clades already present in the south may have jointly promoted the formation of subtropical EBLFs in eastern China since the early Miocene.

Key words: climate, East Asian monsoon, Miocene, niche evolution, *Quercus*.

1 Introduction

The evolution of subtropical evergreen broad-leaved forests (EBLFs) in eastern China has attracted much attention from ecologists and biogeographers during the last decades (Song, 2013; Yu et al., 2017; Chen et al., 2018; Deng et al., 2018; Hai et al., 2022). Subtropical EBLFs, the warm temperate laurophyll forests in the IUCN Global Ecosystem Typology (Keith et al., 2022), are the predominant forest type under the monsoon climate in eastern Asia. They range 23–33° N, 98–123° E in China, covering the south edge of the Himalayas, Hengduan Mountains and eastern China (Song, 2013), and range 26.5–37.5° N in southern Japan (Fujiwara & Box, 1998). However, evidence from palaeobotanical and lithological data across China revealed that in the Paleogene (66.0–23.0 million years ago [Ma]), there was a broad belt of aridity (annual precipitation < 200 mm) stretching across China from west to east; while in the Neogene

(23.0–2.6 Ma), the humid zone (annual precipitation > 500 mm) greatly expanded in eastern China (Wang, 1990; Sun & Wang, 2005; Guo, 2017). The reorganization of the climate system and vegetation pattern in eastern China have been linked to the uplift of the Himalayas during the Cenozoic, strengthened East Asian monsoon during the Miocene (23.0–5.3 Ma), and global cooling after the climatic optimum in the middle Miocene (Guo et al., 2008; Farnsworth et al., 2019). However, the temporal history and main driver of the formation of subtropical EBLFs in eastern China remain mysterious.

The history of subtropical EBLFs can be partially inferred from the phylogeny of their dominant components and the fossils of ancient floras. Reconstruction of time-calibrated phylogenies of some dominant taxa in subtropical EBLFs has shown that most genera had derived before the Miocene, followed by an across-the-board acceleration in net

This is an open access article under the terms of the Creative Commons Attribution-NonCommercial License, which permits use, distribution and reproduction in any medium, provided the original work is properly cited and is not used for commercial purposes.

diversification rates during the Miocene, among which were the family Theaceae (Yu et al., 2017), the Perseeae tribe of the family Lauraceae (Xiao et al., 2022), section *Michelia* of the genus *Magnolia* (Magnoliaceae) (Zhao et al., 2022), and section *Cyclobalanopsis* of the genus *Quercus* (Fagaceae) (Deng et al., 2018). On a larger scale, by investigating the divergence patterns of the Chinese flora, Lu et al. (2018) found that with mean divergence times of 24.1–27.6 Ma, woody genera in eastern China (annual precipitation > 500 mm) were derived mostly in the Oligocene and experienced remarkable acceleration in diversification rates during the Miocene. On the other side, fossils of ancient floras have shown that subtropical or tropical EBLFs already existed in south China during the Eocene, such as Changchang in Hainan, Maoming in Guangdong (Spicer et al., 2014; Herman et al., 2017; Ling et al., 2021), and in southwest China during the early Oligocene, for example, Lvhe Basin, Wenshan Basin in Yunnan, and Ningming in Guangxi (Su et al., 2019; Ling et al., 2021; Tian et al., 2021). In east China, fossil floras from the middle Miocene in Jiangxi (He & Wang, 2021) and from the late Miocene in Zhejiang (Jia et al., 2015; Li et al., 2015; Ding et al., 2021) indicate that subtropical EBLFs existed in

east China during the Miocene. As phylogenies do not directly reflect their relationships with climate elements, and fossil records can only record the history of a few sites, the linkage between species diversification, climate change and the evolution of subtropical EBLFs in eastern China has not been well established.

As a lineage, the *Cyclobalanopsis*, or ring-cupped oaks, have historically been considered either as a genus, or as a subgenus of *Quercus*. Today, based on molecular phylogeny (Denk et al., 2017; Deng et al., 2018), *Cyclobalanopsis* is considered as a section in the subgenus *Cerris* of the genus *Quercus*. Covering about 100 extant species, ring-cupped oaks are evergreen, woody species often dominant in EBLFs in eastern Asia and on Pacific islands (Luo & Zhou, 2001; Denk et al., 2017). With 69 indigenous species, of which 43 are endemic, China is a major center of diversity for *Cyclobalanopsis* (Huang et al., 1999). In Asia, early fossils of *Cyclobalanopsis* were found in Japan (southwest Honshu) from the middle Eocene (Huzioka & Takahasi, 1970), and in south China (Changchang, Hainan), dated to 48.6–37.2 Ma (Liu et al., 2020) (Fig. 1). *Cyclobalanopsis* fossils dated to the Miocene were found as dominant elements in many eastern

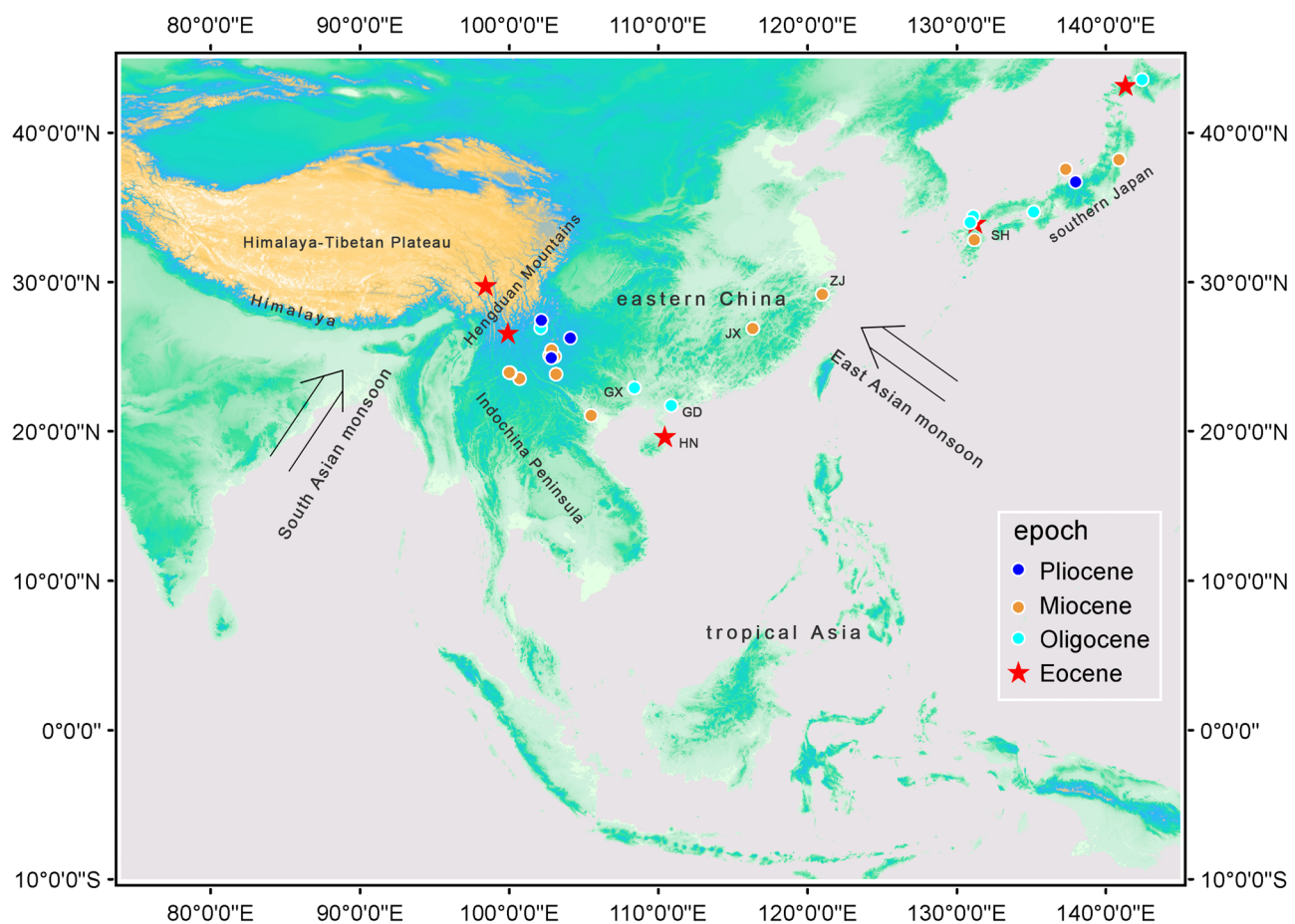


Fig. 1. Fossil records of *Quercus* section *Cyclobalanopsis* in eastern Asia. Abbreviations of fossil sites, HN, Hainan (Spicer et al., 2014; Liu et al., 2020); SH, Southwest Honshu (Huzioka & Takahasi, 1970); GD, Guangdong (Liu et al., 2019); GX, Guangxi (Liu et al., 2023); JX, Jiangxi (He & Wang, 2021); ZJ, Zhejiang (Jia et al., 2015; Jia et al., 2009). The remaining fossil records were compiled from the following references: Gourbet et al. (2017), Guo (1978), Guo (2011), Su et al. (2019), Tanai (1995), Xing et al. (2013), Xu et al. (2016), Yabe (2008), and Zhou (1999).

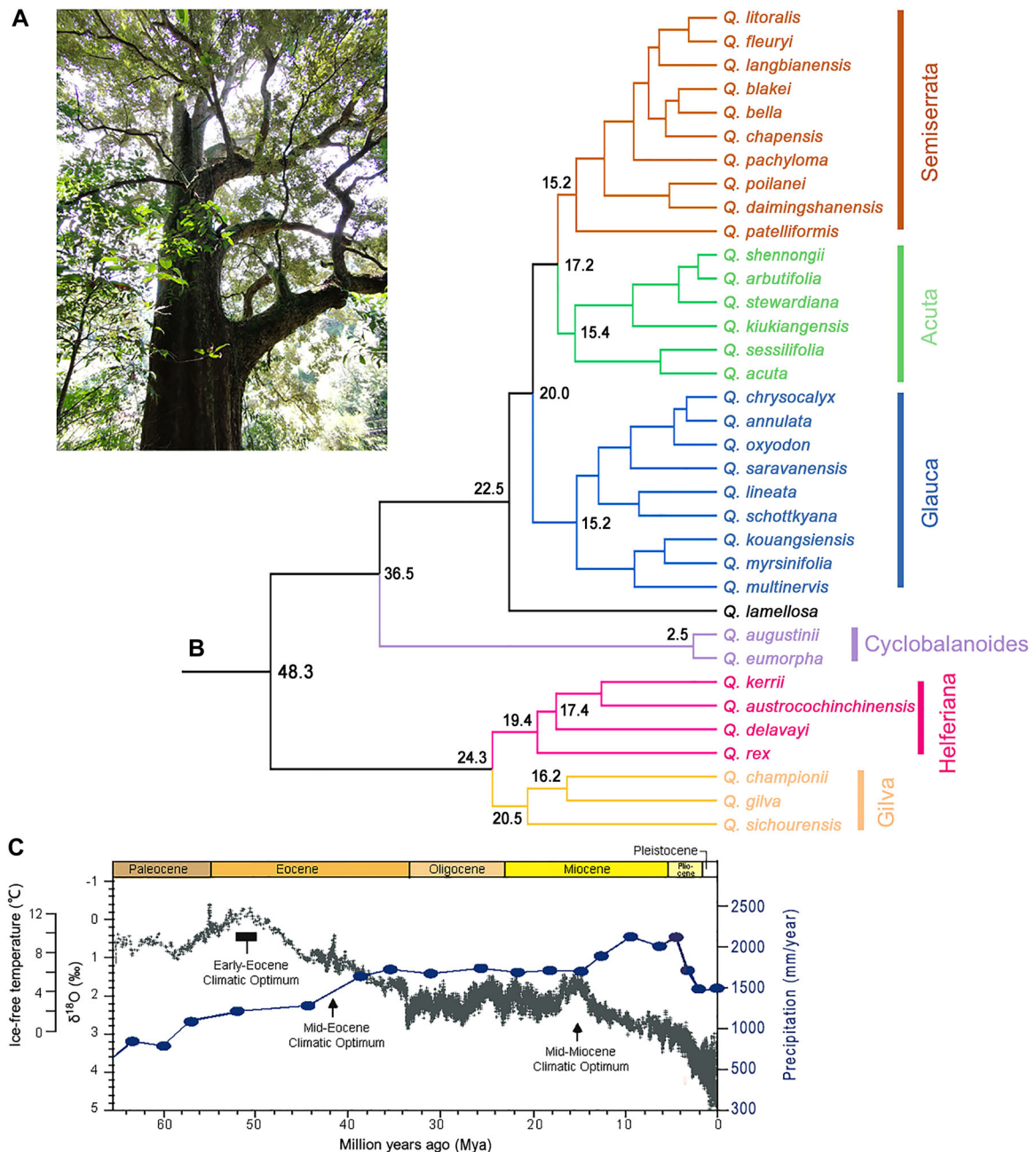


Fig. 2. *Quercus Gilva* as a representative of *Quercus* section *Cyclobalanopsis* (A), recalibrated phylogeny of section *Cyclobalanopsis* from Deng et al. (2018) (B), and the historical change in deep ocean temperatures (Zachos et al., 2008) and modelled mean annual precipitation in eastern Asia (Farnsworth et al., 2019) (C).

Asian floras, including eastern China and southern Japan (Zhou, 1999; Jia et al., 2015). The diversity and importance of *Cyclobalanopsis* in subtropical EBLFs, and their long history in China, make it an ideal taxon to study the evolution of subtropical EBLFs in eastern China.

Here we take *Quercus* section *Cyclobalanopsis* as a representer to clarify the history of subtropical EBLFs in eastern China. When and how did *Cyclobalanopsis* evolve, and what are the key elements that have driven its evolution? To address these questions, we integrated the occurrence data, climate data, and dated phylogeny of 35 *Cyclobalanopsis* species, and applied

ecological niche models and climatic niche analysis. We examined: (i) where *Cyclobalanopsis* species live and how the clades differ in climatic preference, and (ii) when and how the climate tolerances of *Cyclobalanopsis* evolved.

2 Material and Methods

2.1 Phylogeny

In this study we have used the phylogeny of *Quercus* section *Cyclobalanopsis* published by Deng et al. (2018), which was

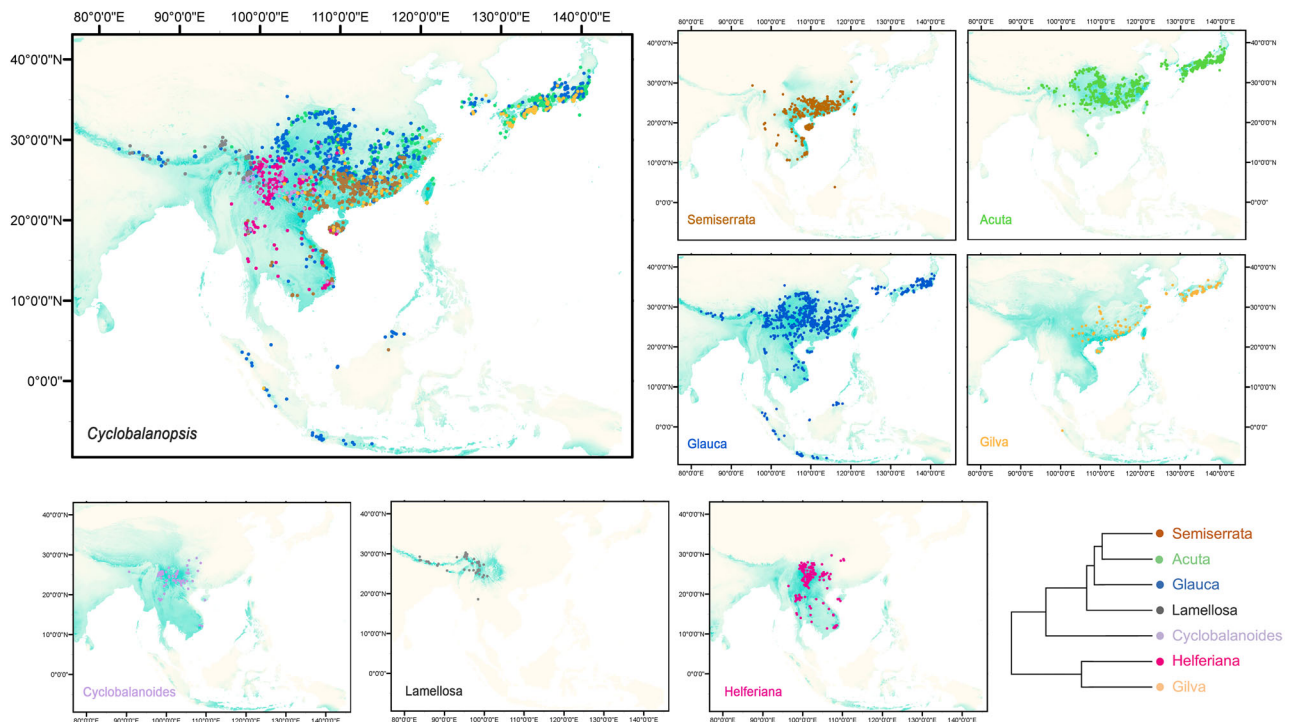


Fig. 3. Geographical distributions of *Cyclobalanopsis* and its seven clades. Occurrence points and species density of each clade were overlapped from occurrences of each species within the clades, and corresponding occurrence possibility predicted by MaxEnt.

constructed based on the restriction site-associated DNA sequencing (RAD-seq) with divergence times estimated using a relaxed clock model. This phylogeny has proportionally presented the diversity of *Cyclobalanopsis* and covered the main clades. It includes 35 *Cyclobalanopsis* species from seven clades, namely *Semiserrata*, *Acuta*, *Glauca*, *Lamellosa*, *Cyclobalanoides*, *Gilva*, and *Helferiana*. Considering that the crown age of *Cyclobalanopsis* in Deng et al. (2018) is 26.26 Ma, which was much more recent than many fossil *Cyclobalanopsis* species dated to the middle Eocene (Huzioka & Takahasi, 1970; Manchester, 1994; Liu et al., 2020), we recalibrated this phylogeny using 48.32 Ma as the crown age instead (Manchester, 1994; Hipp et al., 2020). The recalibrated phylogeny of *Quercus* section *Cyclobalanopsis* is shown in Fig. 2, along with the modeled histories of temperature and precipitation of eastern Asia since the Paleocene (Zachos et al., 2008; Farnsworth et al., 2019).

2.2 Species occurrence and the climate data

Occurrence data of the 35 *Cyclobalanopsis* species in the phylogeny were compiled from species occurrences from the Global Biodiversity Information Facility (GBIF), records of our fieldwork, as well as specimen information from the Chinese Virtual Herbarium (CVH) and the Chinese Field Herbarium (CFH). We checked the data for each species, and removed duplicates, artificial plantations, and other unlikely locations. No more than one occurrence was kept in each grid of 2.5×2.5 arc min. Finally, we got 2924 occurrences of the 35 *Cyclobalanopsis* species for analysis (Data S1).

We downloaded 19 bioclimatic factors of WorldClim (version 2.1) for 1970–2000 with a spatial resolution of 2.5 arc min (Fick & Hijmans, 2017). All the 19 climatic factors and elevation for each of the 2924 occurrences were queried by location (Data S1).

2.3 Niche modeling

Climatic niche modeling for each of the 35 *Cyclobalanopsis* species (Fig. S1) was carried out using MaxEnt (version 3.4.4) (Phillips & Dudik, 2008), setting autofeatures with 10 replicates. Seven bioclimatic layers with pairwise Pearson's correlation coefficients less than 0.8 were kept for niche modeling: (i) mean diurnal range (bio2); (ii) temperature seasonality (bio4); (iii) max temperature of warmest month (bio5); (iv) minimum temperature of coldest month (bio6); (v) mean temperature of wettest quarter (bio8); (vi) precipitation of wettest quarter (bio16); and (vii) precipitation of driest quarter (bio17). The average area under the curve under the receiver operating characteristic curve for niche modeling of the 35 species was 0.96 with the range 0.89–0.98 (Table S1). Permutation importance and predicted niche occupancy of each climatic variable for each species were acquired from the results of niche modeling.

2.4 Analysis of climatic niche evolution

To determine the essential climatic factors in the evolution of *Cyclobalanopsis*, all 19 factors were analyzed for niche evolution. We applied disparity through time and the morphological disparity index (MDI) to describe the history of climatic niche evolution of *Quercus* section *Cyclobala-*

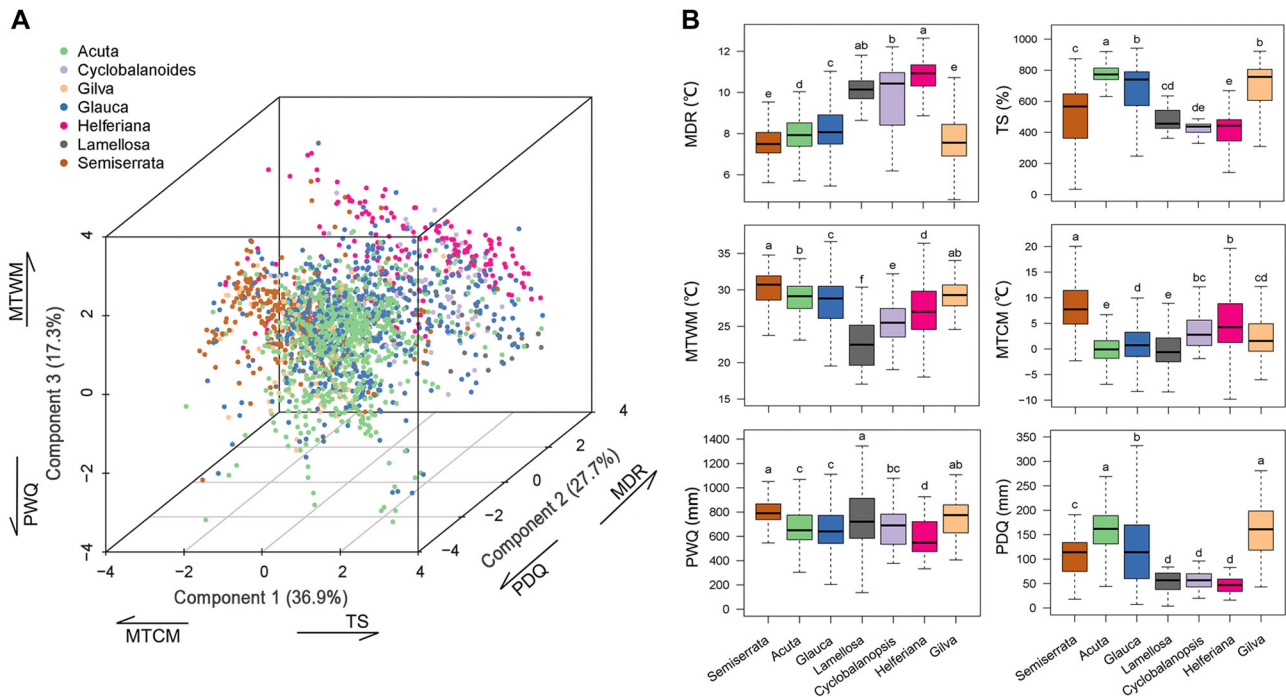


Fig. 4. Three-dimensional principal component analysis (3D-PCA) for *Quercus* section *Cyclobalanopsis* using six climatic factors and 2924 occurrences of 35 species (A) and comparisons of the climatic tolerances among seven clades using Turkey HSD (B). Clades with the same letter are not significantly different at $P < 0.05$ level. MDR, mean diurnal range; MTCM, min temperature of coldest month; MTWM, max temperature of warmest month; PDQ, precipitation of driest quarter; PWQ, precipitation of wettest quarter; TS, temperature seasonality. Loadings of each climatic factor on the first three principal components are shown in Table S1.

nopsis. Disparity, representing average squared Euclidean distance among all pairs of terminal taxa at each node of the phylogeny, was compared with the mean disparity of an unconstrained model of Brownian evolution. MDI represents the overall difference in disparity between the observed and the unconstrained null hypothesis for each climatic factor. Disparity through time with MDI for each climatic factor was analyzed using “dtt” in the *geiger* package (Pennell et al., 2014). We also calculated Blomberg’s K of phylogenetic signal for each climatic factors with “phylosignal” in package *picante* (Kembel et al., 2010). For ancestral climatic tolerances, we calculated the generalized-least-squares estimate for each climate variable at each interior node and repeated this process using 1000 random samples from the niche occupancy profiles for the extant taxa. Ancestral climatic tolerances were estimated using “anc.clim” in the *phyloclim* package (Evans et al., 2009). All these analyses were carried out in R (version 4.3.0) (R Core Team, 2023).

3 Results

3.1 The western and eastern groups in *Cyclobalanopsis*

Overlapped occurrences and niche modeling of *Cyclobalanopsis* (Fig. 3) are consistent with the range of subtropical and tropical EBLFs in eastern Asia, covering the south edge of the Himalayas, the Hengduan Mountains, Indochina Peninsula, eastern China, the southernmost part of the Korean Peninsula, and southern

Japan. Clades *Cyclobalanoides*, *Lamellosa*, and *Helderiana* occur mainly in the west, with a mean elevation at occurrence sites of 1659 m.a.s.l., they mainly inhabit the south edge of the Himalayas, the Hengduan Mountains, and Indochina Peninsula. Clades *Semiserrata*, *Acuta*, *Glauca*, and *Gilva* occupy a vast area in the east, with a mean elevation at occurrence sites of 674 m.a.s.l., they are mainly distributed in eastern China, and southern Japan. Principal component analysis of seven climatic factors of 35 species (Fig. 4A; Table S2) also showed that all the occurrences can be roughly divided into two groups, corresponding to the western and the eastern groups. By comparing the climatic factors among clades using Tukey’s honestly significant difference (Tukey HSD; Figs. 4B, S2), we found that habitats of the eastern clades were higher in precipitation of driest/coldest quarter and maximum temperature of warmest month/quarter but were lower in mean diurnal range, precipitation seasonality, and isothermality than that of the western clades ($P < 0.05$). For precipitation of the wettest/warmest quarter, there was no such obvious difference between the eastern and western groups.

3.2 Disparities of climatic tolerances of *Cyclobalanopsis* since the early Miocene

Disparities of 19 climatic tolerances of *Cyclobalanopsis* in comparison with simulated patterns under Brownian motion through evolutionary history are shown in Figs.

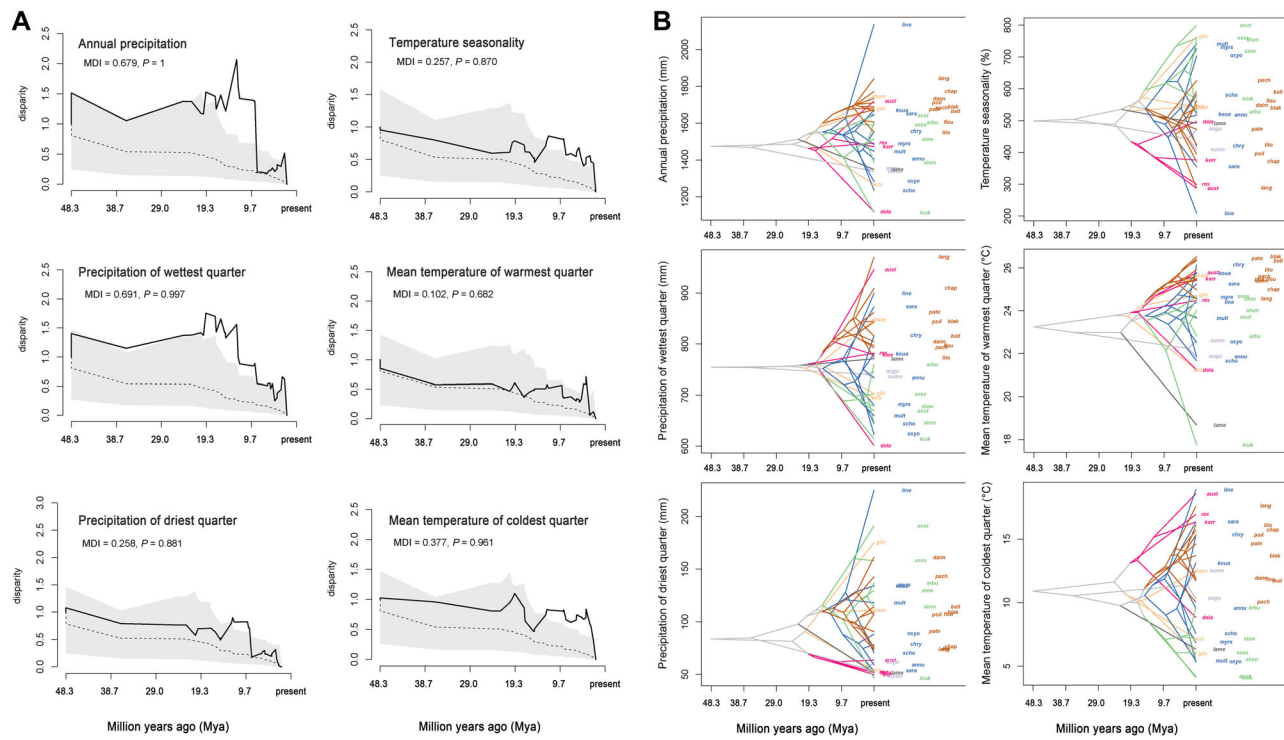


Fig. 5. Disparity through time (A) and reconstructed ancestral tolerances (B) of three precipitation elements and three temperature elements of *Quercus* section *Cyclobalanopsis*. In (A), the solid line shows the disparity among all pairs of terminal taxa at each node of the phylogeny, the dashed line shows mean disparity of an unconstrained model of Brownian evolution and the gray cloud shows 95% confidence interval. The morphological disparity index (MDI) value represents the overall difference in disparity between the observed and the unconstrained null hypothesis. In (B), names of extant species were abbreviated using the first four letters in the same color with the clade as in Fig. 2.

5A, S3, and Table 1. Four precipitation-related factors (precipitation of warmest quarter, wettest quarter, wettest month, and annual precipitation) showed significantly larger disparities than those under Brownian motion ($P < 0.05$). These disparities of precipitation elements were remarkably enhanced during the Miocene. When we removed all but three clades, *Semiserrata*, *Acuta*, and *Glauca*, in the phylogeny, the above pattern did not change (Table 1). The mean temperature of the driest/coldest quarter also showed enhanced disparities in the *Cyclobalanopsis* section. Unlike the above elements, factors, such as mean diurnal range, isothermality, mean temperature of warmest quarter, precipitation seasonality, and precipitation of the driest/coldest quarter, showed a larger Blomberg's K and significant phylogenetic signal ($P < 0.05$).

3.3 Divergence of climatic tolerance of *Cyclobalanopsis* since the early Miocene

Reconstruction of the evolutionary history of climatic tolerances in *Quercus* section *Cyclobalanopsis*, see Figs. 5B and S4, showed that significant divergence occurred mainly in the past 19 Ma, since the early Miocene. The eastern clades *Semiserrata*, *Acuta*, and *Glauca* showed strong innovation in climate tolerance to a higher precipitation in the driest/coldest quarter, to a lower precipitation seasonality, and to a lower mean diurnal range. For precipitations of the warmest

quarter and annual precipitation, intersections among the clades are very common.

4 Discussion

4.1 The origin of *Quercus* section *Cyclobalanopsis* in Asia

Our niche modeling of extant species has shown that early derived clades and species in *Cyclobalanopsis*, for example, clades *Cyclobalanoides* and *Lamellosa* (Fig. 3), species *Quercus patelliformis*, and *Quercus rex* (Fig. S1) are usually inhabitants of the Himalaya–Hengduan region of southwest China, south China, and the coastal region of the west Pacific. This result is in accordance with the fossil records (Fig. 1) that ancient *Cyclobalanopsis* occurred in south China, Japan, and the Himalaya–Hengduan region in the Eocene and the Oligocene (Huzioka & Takahasi, 1970; Zhou, 1999; Xu et al., 2016; Liu et al., 2019, 2023). Although the modern Himalaya–Hengduan region is a mountainous area, it was on the coast of the Tethys Ocean before the collision of the Indian and Eurasian Plates (Royden et al., 2008; Ding et al., 2017). We infer that ancient *Cyclobalanopsis* may have been widely distributed in the coastal regions of the western Pacific and the Tethys Ocean during the Eocene, which is similar to its sister clade *Quercus* section *Illex* (Jiang et al., 2019), when the climate was much warmer than both during the Miocene and today (Sun & Wang, 2005; Zachos et al., 2008).

Table 1 Morphological disparity index (MDI) and Blomberg's *K* of 19 climatic elements in *Quercus* section *Cyclobalanopsis* (MDI and *K*) and the subclade including *Semiserrata*, *Acuta*, and *Glauca* (MDI' and *K*').

Climatic factor	MDI	<i>K</i>	MDI'	<i>K</i> '
Precipitation of warmest quarter (bio18)	1.29	0.17	0.76	0.34
Precipitation of wettest quarter (bio16)	0.69	0.29	0.38	0.50
Annual precipitation (bio12)	0.68	0.34	0.71	0.44
Precipitation of wettest month (bio13)	0.64	0.27	0.43	0.45
Mean temperature of driest quarter (bio9)	0.41	0.29	0.23	0.58
Mean temperature of coldest quarter (bio11)	0.38	0.30	0.21	0.58
Max temperature of warmest month (bio5)	0.35	0.33	0.26	0.52
Annual mean temperature (bio1)	0.33	0.32	0.18	0.60
Min temperature of coldest month (bio6)	0.33	0.29	0.25	0.55
Temperature annual range (bio7)	0.26	0.28	0.24	0.56
Precipitation of driest quarter (bio17)	0.26	0.46	0.22	0.73
Temperature seasonality (bio4)	0.26	0.32	0.22	0.58
Precipitation of driest month (bio14)	0.25	0.45	0.20	0.73
Precipitation seasonality (bio15)	0.21	0.44	0.17	0.69
Precipitation of coldest quarter (bio19)	0.20	0.44	0.28	0.62
Mean diurnal range (bio2)	0.15	0.71	0.22	0.65
Isothermality (bio3)	0.13	0.39	0.19	0.66
Mean temperature of wettest quarter (bio8)	0.12	0.34	0.22	0.55
Mean temperature of warmest quarter (bio10)	0.10	0.43	0.19	0.57

MDI and *K* values with a corresponding *P*-value < 0.05 are shown in bold type.

4.2 Divergence between the western and eastern groups in *Cyclobalanopsis*

Cyclobalanopsis species can be divided into two groups with significant divergence in both geological distribution and climatic tolerance. Along with the uplift of the Himalaya orogen, the western clades, *Lamellosa*, *Cyclobalanoides*, and *Helferiana*, may have gradually adapted to the plateau climate under the control of the South Asian monsoon (Gupta et al., 2015; Spicer, 2017), which is characterized by a wide range of daily temperatures, a cooler summer, and high

precipitation seasonality. For the eastern clades, which occupy a vast area under the influence of the East Asian monsoon in summer and the Siberian Cold Current in winter, they have adapted to a climate of hot summers, wet winters, and low precipitation seasonality. In addition, we observed that for both ancient and extant species, *Cyclobalanopsis* can grow at latitudes about 5° higher in Japan than in eastern China. This phenomenon is largely due to the Kuroshio Current, the biggest current in the western Pacific, that transports large amounts of heat to southern Japan (Nagai et al., 2019).

4.3 Diversification of subtropical EBLFs in eastern China since the early Miocene

The rapid *Cyclobalanopsis* speciation (especially in the eastern clades) that began 19 Ma in the early Miocene has been accompanied by climatic niche innovation and divergence in climate tolerance, which is supported by the disparity of climatic tolerances through the history and the reconstructed ancestral tolerances in *Cyclobalanopsis* (Fig. 5). For other dominant clades in subtropical EBLFs, the family Theaceae showed sharp rises around 20 Ma in both speciation rate and net diversification rate (Yu et al., 2017); the Perseeae tribe of the family Lauraceae began to colonize the subtropical EBLFs in the early Miocene (Xiao et al., 2022); and section *Michelia* of the genus *Magnolia* diversified in their subtropical clades mainly since the late Miocene (Zhao et al., 2022). As the major clades of subtropical EBLFs in eastern China, such as *Quercus* section *Cyclobalanopsis*, occupied new niche space in eastern China and expanded their range in local habitats, species diversification and climatic tolerance innovation occurred simultaneously.

4.4 Enhanced precipitation as the essential driver for subtropical EBLFs in eastern China

The enhanced MDIs (Figs. 5A, S3; Table 1) and the reconstructed evolutionary history (Figs. 5B, S4) indicated that *Cyclobalanopsis* clades, especially the recent eastern clades, radiated simultaneously to precipitation of the warmest/wettest quarter and to annual precipitation during the Miocene. Meanwhile, with relatively higher *K* values and significant phylogeny signals (Table 1), *Cyclobalanopsis* species showed phylogenetically conservative in some climatic factors, for example, mean diurnal range, isothermality and precipitation seasonality. In the context of the dramatic transition from the arid Paleogene to the humid Neogene in eastern China as revealed by paleobotanical records (Sun & Wang, 2005; Guo et al., 2008), and the significant enhancement of mean annual precipitation in eastern Asia during the Miocene (Farnsworth et al., 2019), we may infer that the strengthened East Asian monsoon had radically changed the environment in eastern China, creating vast, vacant niche space for various evergreen woody species during the early Miocene. The establishment of the East Asian monsoon system at the Oligocene–Miocene boundary (Sun & Wang, 2005; Guo et al., 2008), may have promoted the subsequent evolution and expansion of subtropical EBLFs in eastern China; while the uplift of Himalaya–Tibetan Plateau, and global cooling (Guo, 2017; Spicer, 2017; Farnsworth et al., 2019) may have induced the intensification

of the East Asian monsoon system and thus promoted the evolution of subtropical EBLFs indirectly.

Overall, our research establishes a link between species diversification, niche evolution and enhanced precipitation in *Cyclobalanopsis*, as well as in subtropical EBLFs in eastern China. We conclude that, driven by the enhanced East Asian monsoon, subtropical EBLFs in eastern China have greatly increased in diversity and expanded in geographical range since the early Miocene. Species diversification and occupation of new climatic niches by the ancient clades already present in southwest China, south China and tropical Asia may have jointly promoted the formation of subtropical EBLFs in eastern China.

Acknowledgements

We thank Prof. Min Deng of Yunnan University, Prof. Li-mi Mao from Nanjing Institute of Geological and Palaeontology, CAS, and Dr. Meng-Xiao Yan of Shanghai Chenshan Botanical Garden for helpful suggestions. We are grateful to Ms. Béatrice Chassé of the International Oak Society who has carefully checked and improved the language. This research was funded by the National Natural Science Foundation of China (No. 31901217), and the Special Fund for Scientific Research of Shanghai Landscaping & City Appearance Administrative Bureau (No. G192422).

References

- Chen YS, Deng T, Zhou Z, Sun H. 2018. Is the East Asian flora ancient or not? *National Science Review* 5: 920–932.
- Deng M, Jiang XL, Hipp AL, Manos PS, Hahn M. 2018. Phylogeny and biogeography of East Asian evergreen oaks (*Quercus* section *Cyclobalanopsis*; Fagaceae): Insights into the Cenozoic history of evergreen broad-leaved forests in subtropical Asia. *Molecular Phylogenetics and Evolution* 119: 170–181.
- Denk T, Grimm GW, Manos PS, Deng M, Hipp AL. 2017. An updated infrageneric classification of the oaks: Review of previous taxonomic schemes and synthesis of evolutionary patterns. In: Gil-Pelegrín E, Peguero-Pina J, Sancho-Knapik D eds. *Oaks physiological ecology. Exploring the functional diversity of genus Quercus L.* Tree physiology. Cham, Switzerland: Springer. 7: 12–38.
- Ding L, Spicer RA, Yang J, Xu Q, Cai F, Li S, Lai Q, Wang H, Spicer TEV, Yue Y, Shukla A, Srivastava G, Khan MA, Bera S, Mehrotra R. 2017. Quantifying the rise of the Himalaya orogen and implications for the South Asian monsoon. *Geology* 45: 215–218.
- Ding ST, Wu JY, Tang DL, Chen SY, Mo LB, Sun BN. 2021. Seed cones of *Tsuga* (Pinaceae) from the upper Miocene of eastern China: Biogeographic and paleoclimatic implications. *Review of Palaeobotany and Palynology* 285: 104358.
- Evans MEK, Smith SA, Flynn RS, Donoghue MJ. 2009. Climate, niche evolution, and diversification of the “bird-cage” evening primroses (*Oenothera*, Sections *Anogra* and *Kleinia*). *American Naturalist* 173: 225–240.
- Farnsworth A, Lunt DJ, Robinson SA, Valdes PJ, Roberts WHG, Clift PD, Markwick P, Su T, Wrobel N, Bragg F, Kelland SJ, Pancost RD. 2019. Past East Asian monsoon evolution controlled by paleogeography, not CO₂. *Science Advances* 5: eaax1697.
- Fick SE, Hijmans RJ. 2017. WorldClim 2: New 1-km spatial resolution climate surfaces for global land areas. *International Journal of Climatology* 37: 4302–4315.
- Fujiwara K, Box EO 1998. Evergreen broad-leaved forests in Japan and eastern north America: Vegetation shift under climatic warming. In: Klotzli F, Walther GR eds. *Conference on recent shifts in vegetation boundaries of deciduous forests, especially due to general global warming*. Ascona: Birkhauser. 273–300
- Gourbet L, Leloup PH, Paquette JL, Sorrel P, Maheo G, Wang G, Yadong X, Cao K, Antoine PO, Eymard I, Liu W, Lu H, Replumaz A, Chevalier ML, Kexin Z, Jing W, Shen T. 2017. Reappraisal of the Jianchuan Cenozoic basin stratigraphy and its implications on the SE Tibetan plateau evolution. *Tectonophysics* 700–701: 162–179.
- Guo SX. 1978. Pliocene floras of western Sichuan. *Acta Palaeontologica Sinica* 17: 343–350. (in Chinese).
- Guo SX. 2011. The late Miocene Bangmai flora from Lincang County of Yunnan, southwestern China. *Acta Palaeontologica Sinica* 50: 353–408. (in Chinese).
- Guo ZT. 2017. Loess Plateau attests to the onsets of monsoon and deserts. *Scientia Sinica Terrae* 47: 421–437. (in Chinese).
- Guo ZT, Sun B, Zhang ZS, Peng SZ, Xiao GQ, Ge JY, Hao QZ, Qiao YS, Liang MY, Liu JF, Yin QZ, Wei JJ. 2008. A major reorganization of Asian climate by the early Miocene. *Climate of the Past* 4: 153–174.
- Gupta AK, Yuvaraja A, Prakasam M, Clemens SC, Velu A. 2015. Evolution of the South Asian monsoon wind system since the late Middle Miocene. *Palaeogeography Palaeoclimatology Palaeoecology* 438: 160–167.
- Hai L, Li XQ, Zhang JB, Xiang XG, Li RQ, Jabbour F, Ortiz RDC, Lu AM, Chen ZD, Wang W. 2022. Assembly dynamics of East Asian subtropical evergreen broadleaved forests: New insights from the dominant Fagaceae trees. *Journal of Integrative Plant Biology* 64: 2126–2134.
- He WL, Wang XJ. 2021. A Miocene flora from the Toupai Formation in Jiangxi Province, southeastern China. *Palaeoworld* 30: 757–769.
- Herman AB, Spicer RA, Aleksandrova GN, Yang J, Kodrul TM, Maslova NP, Spicer TEV, Chen G, Jin JH. 2017. Eocene–early Oligocene climate and vegetation change in southern China: Evidence from the Maoming Basin. *Palaeogeography, Palaeoclimatology, Palaeoecology* 479: 126–137.
- Hipp AL, Manos PS, Hahn M, Avishai M, Bodenies C, Cavender-Bares J, Crowl AA, Deng M, Denk T, Fitz-Gibbon S, Gailing O, Gonzalez-Elizondo MS, Gonzalez-Rodriguez A, Grimm GW, Jiang XL, Kremer A, Lesur I, McVay JD, Plomion C, Rodriguez-Correa H, Schulze ED, Simeone MC, Sork VL, Valencia-Avalos S. 2020. Genomic landscape of the global oak phylogeny. *New Phytologist* 226: 1198–1212.
- Huang C, Zhang Y, Bartholomew B. 1999. Fagaceae. In: Wu ZY, Raven PH, Hong DY eds. *Flora of China*. Beijing: Science Press. 380–400.
- Huzioka K, Takahasi E. 1970. The Eocene flora of the Ube coal-field, southwest Honshu, Japan. *Journal of the Mining College, Akita University, Series A, Mining Geology* 4: 1–88.
- Jia H, Jin P, Wu J, Wang Z, Sun B. 2015. *Quercus* (subg. *Cyclobalanopsis*) leaf and cupule species in the late Miocene of eastern China and their paleoclimatic significance. *Review of Palaeobotany and Palynology* 219: 132–146.
- Jia H, Sun B, Li X, Xiao L, Wu J. 2009. Microstructures of one species of *Quercus* from the Neogene in Eastern Zhejiang and its palaeoenvironmental indication. *Earth Science Frontiers* 16: 79–90.
- Jiang XL, Hipp AL, Deng M, Su T, Zhou ZK, Yan MX. 2019. East Asian origins of European holly oaks (*Quercus* section *Ilex* Loudon) via the Tibet-Himalaya. *Journal of Biogeography* 46: 2203–2214.
- Keith DA, Ferrer-Paris JR, Nicholson E, Bishop MJ, Polidoro BA, Ramirez-Llodra E, Tozer MG, Nel JL, Nally RM, Gregr EJ,

- Watermeyer KE, Essl F, Faber-Langendoen D, Franklin J, Lehmann CER, Etter A, Roux DJ, Stark JS, Rowland JA, Brummitt NA, Fernandez-Arcaya UC, Suthers IM, Wisser SK, Donohue I, Jackson LJ, Pennington RT, Iliffe TM, Gerovasileiou V, Giller P, Robson BJ, Pettorelli N, Andrade A, Lindgaard A, Tahvanainen T, Terauds A, Chadwick MA, Murray NJ, Moat J, Plissock P, Zager I, Kingsford RT. 2022. A function-based typology for Earth's ecosystems. *Nature* 610: 513–518.
- Kembel SW, Cowan PD, Helmus MR, Cornwell WK, Morlon H, Ackerly DD, Blomberg SP, Webb CO. 2010. Picante: R tools for integrating phylogenies and ecology. *Bioinformatics* 26: 1463–1464.
- Li R, Sun B, Wang Q, Ma F, Xu X, Wang Y, Jia H. 2015. Two new *Castanopsis* (Fagaceae) species based on cupule and foliage from the upper Miocene of eastern Zhejiang, China. *Plant Systematics and Evolution* 301: 25–39.
- Ling CC, Ma FJ, Dong JL, Zhou GH, Wang QJ, Sun BN. 2021. A mid-altitude area in southwestern China experienced a humid subtropical climate with subtle monsoon signatures during the early Oligocene: Evidence from the Ningming flora of Guangxi. *Palaeogeography Palaeoclimatology Palaeoecology* 579: 110601.
- Liu X, Song H, Jin J. 2020. Diversity of Fagaceae on Hainan Island of South China during the Middle Eocene: Implications for phytogeography and paleoecology. *Frontiers in Ecology and Evolution* 8: 225.
- Liu XY, Song HZ, Wu XK, Hu JR, Huang WY, Quan C, Jin JH. 2023. Late Oligocene fossil acorns and nuts of *Quercus* section *Cyclobalanopsis* from the Nanning Basin, Guangxi, South China. *Plant Diversity* 45: 434–445.
- Liu XY, Xu SL, Han MQ, Jin J. 2019. An early Oligocene fossil acorn, associated leaves and pollen of the ring-cupped oaks (*Quercus* subg. *Cyclobalanopsis*) from Maoming Basin, South China. *Journal of Systematics and Evolution* 57: 153–168.
- Lu LM, Mao LF, Yang T, Ye JF, Liu B, Li HL, Sun M, Miller JT, Mathews S, Hu HH, Niu YT, Peng DX, Chen YH, Smith SA, Chen M, Xiang KL, Le CT, Dang VC, Lu AM, Soltis PS, Soltis DE, Li JH, Chen ZD. 2018. Evolutionary history of the angiosperm flora of China. *Nature* 554: 234–238.
- Luo Y, Zhou ZK. 2001. Phytogeography of *Quercus* subg. *Cyclobalanopsis*. *Acta Botanica Yunnanica* 23: 1–16.
- Manchester SR. 1994. Fruits and seeds of the middle eocene nut beds flora Clarno Formation, Oregon. *Palaeontographica Americana* 58: 1–205.
- Nagai T, Saito H, Suzuki K, Takahashi M eds. 2019. *Kuroshio current: Physical, biogeochemical, and ecosystem dynamics*. Hoboken, NJ: Wiley. 3–50
- Pennell MW, Eastman JM, Slater GJ, Brown JW, Uyeda JC, FitzJohn RG, Alfaro ME, Harmon LJ. 2014. geiger v2.0: An expanded suite of methods for fitting macroevolutionary models to phylogenetic trees. *Bioinformatics* 30: 2216–2218.
- Phillips SJ, Dudik M. 2008. Modeling of species distributions with Maxent: new extensions and a comprehensive evaluation. *Ecography* 31: 161–175.
- R Core Team. 2023. *R: A language and environment for statistical computing*. Vienna: R Foundation for Statistical Computing. Available from <http://www.r-project.org>
- Royden LH, Burchfiel BC, van der Hilst RD. 2008. The geological evolution of the Tibetan plateau. *Science* 321: 1054–1058.
- Song Y. 2013. *Evergreen broadleaved forests in China, classification-ecology-conservation*. Beijing: Science Press. 3–9 (in Chinese).
- Spicer RA. 2017. Tibet, the Himalaya, Asian monsoons and biodiversity—In what ways are they related? *Plant Diversity* 39: 233–244.
- Spicer RA, Herman AB, Liao W, Spicer TEV, Kodrul TM, Yang J, Jin JH. 2014. Cool tropics in the Middle Eocene: Evidence from the Changchang Flora, Hainan Island, China. *Palaeogeography, Palaeoclimatology, Palaeoecology* 412: 1–16.
- Su T, Spicer RA, Li SH, Xu H, Huang J, Sherlock S, Huang YJ, Li SF, Wang L, Jia LB, Deng WYD, Liu J, Deng CL, Zhang ST, Valdes PJ, Zhou ZK. 2019. Uplift, climate and biotic changes at the Eocene-Oligocene transition in south-eastern Tibet. *National Science Review* 6: 495–504.
- Sun XJ, Wang PX. 2005. How old is the Asian monsoon system? Palaeobotanical records from China. *Palaeogeography Palaeoclimatology Palaeoecology* 222: 181–222.
- Tanai T. 1995. Fagaceous leaves from the Paleogene of Hokkaido, Japan. *Bulletin of the National Science Museum Series C (Geology and Paleontology)* 21: 71–101.
- Tian Y, Spicer RA, Huang J, Zhou Z, Su T, Widdowson M, Jia L, Li S, Wu W, Xue L, Luo P, Zhang S. 2021. New early oligocene zircon U-Pb dates for the 'Miocene' Wenshan Basin, Yunnan, China: Biodiversity and paleoenvironment. *Earth and Planetary Science Letters* 565: 116929.
- Wang PX. 1990. Neogene stratigraphy and paleoenvironments of China. *Palaeogeography Palaeoclimatology Palaeoecology* 77: 315–334.
- Xiao TW, Yan HF, Ge XJ. 2022. Plastid phylogenomics of tribe Perseeae (Lauraceae) yields insights into the evolution of East Asian subtropical evergreen broad-leaved forests. *BMC Plant Biology* 22: 32.
- Xing Y, Hu J, Jacques FMB, Wang L, Su T, Huang Y, Liu YS, Zhou Z. 2013. A new *Quercus* species from the upper Miocene of southwestern China and its ecological significance. *Review of Palaeobotany and Palynology* 193: 99–109.
- Xu H, Su T, Zhang ST, Deng M, Zhou ZK. 2016. The first fossil record of ring-cupped oak (*Quercus* L. subgenus *Cyclobalanopsis* (Oersted) Schneider) in Tibet and its paleoenvironmental implications. *Palaeogeography Palaeoclimatology Palaeoecology* 442: 61–71.
- Yabe A. 2008. Early Miocene terrestrial climate inferred from plant megafossil assemblages of the Joban and Soma areas, Northeast Honshu, Japan. *Bulletin of the Geological Survey of Japan* 59: 397–413.
- Yu XQ, Gao LM, Soltis DE, Soltis PS, Yang JB, Fang L, Yang SX, Li DZ. 2017. Insights into the historical assembly of East Asian subtropical evergreen broadleaved forests revealed by the temporal history of the tea family. *New Phytologist* 215: 1235–1248.
- Zachos JC, Dickens GR, Zeebe RE. 2008. An early Cenozoic perspective on greenhouse warming and carbon-cycle dynamics. *Nature* 451: 279–283.
- Zhao N, Park S, Zhang YQ, Nie ZL, Ge XJ, Kim S, Yan HF. 2022. Fingerprints of climatic changes through the late Cenozoic in southern Asian flora: *Magnolia* section *Michelia* (Magnoliaceae). *Annals of Botany* 130: 41–52.
- Zhou ZK. 1999. Fossils of the Fagaceae and their implications in systematics and biogeography. *Acta Phytotaxonomica Sinica* 37: 369–385. (in Chinese).

Supplementary Material

The following supplementary material is available online for this article at <http://onlinelibrary.wiley.com/doi/10.1111/jse.13022/supinfo>:

Data S1. Occurrences, elevation, and climatic factors of 35 species in *Quercus* section *Cyclobalanopsis*.

Fig. S1. Potential distributions of 35 *Cyclobalanopsis* species predicted using MaxEnt.

Fig. S2. Comparisons of the climatic factors and elevation of occurrences among clades in addition to Fig. 4B.

Fig. S3. Disparity through time of 13 climatic factors in addition to Fig. 5A.

Fig. S4. Reconstructed ancestral climatic tolerances in addition to Fig. 5B.

Table S1. Sample sizes, area under the curve values and permutation importance of each variable for 35 *Cyclobalanopsis* species in ecological modeling using MaxEnt.

Table S2. Loadings of each climatic factor on the first three principal components.